ISSN: 2278-4632
Vol-10 Issue-11 No.03 November 2020

Bio-Inspired Design of Aerodynamic Surfaces for Reduced Drag and Increased Efficiency

[1]B Ramya, [2]T Anuradha, [3]Bhimappa Y

[1,2, 3] Assistant Professor, Department of ME, Narsimha Reddy Engineering College, Secunderabad, Telangana

Abstract

This research investigates the transformative potential of bio-inspired design principles in the realm of aerodynamics, with a specific focus on crafting surfaces that mimic nature's solutions to achieve reduced drag and heightened efficiency. As the demand for sustainable transportation solutions grows, drawing inspiration from evolutionary-honed adaptations in the natural world becomes increasingly relevant. This abstract provides a succinct overview of the study's objectives, methodologies, and key findings. The exploration encompasses a diverse range of biomimetic approaches, from streamlined shapes inspired by avian flight to surface textures influenced by aquatic organisms. The integration of bio-inspired design principles holds the promise of revolutionizing aerodynamic engineering, contributing to the development of more energy-efficient and environmentally friendly vehicles. By delving into the intricacies of biomimicry in aerodynamics, this research aims to pave the way for innovative solutions that transcend traditional engineering boundaries.

1. Introduction

The global pursuit of sustainable and efficient transportation solutions has become a driving force in contemporary engineering, pushing researchers and practitioners to explore unconventional approaches. Among these, the integration of bio-inspired design principles into aerodynamics has garnered significant attention. The natural world, through millions of years of evolution, has developed streamlined and energy-efficient solutions to challenges that parallel those faced by the transportation industry. This exploration delves into the burgeoning field of biomimicry in aerodynamics, focusing on the design of surfaces that draw inspiration from nature's optimization strategies to achieve reduced drag and increased overall efficiency.

The context for the study, underscoring the increasing demand for sustainable transportation solutions. With concerns about environmental impact and the need for improved fuel efficiency, the traditional boundaries of aerodynamic engineering are being challenged. Nature, as an unparalleled source of inspiration, offers a repository of refined designs honed through the iterative process of evolution. This section introduces the overarching goal of the research: to uncover and apply bio-inspired principles in the design of aerodynamic surfaces to enhance efficiency and reduce drag.

ISSN: 2278-4632
Vol-10 Issue-11 No.03 November 2020

As industries seek innovative solutions, biomimicry emerges as a compelling avenue. The section navigates through the motivations behind this shift, highlighting the potential transformative impact on diverse sectors, from aviation to ground transportation. By understanding and emulating nature's solutions, researchers anticipate the development of more streamlined and energy-efficient vehicles. This introduction sets the stage for a journey into the methodologies employed in bio-inspired aerodynamic design, emphasizing the interdisciplinary nature of this field and the multifaceted challenges it aims to address.

Further this section delves into the methodologies underpinning the bio-inspired design of aerodynamic surfaces. Drawing inspiration from the flight dynamics of birds, the streamlined shapes of fish, and the intricate patterns found in insects, researchers seek to translate these adaptations into practical and innovative solutions. Computational modeling, wind tunnel experiments, and advanced materials science are integral components of this exploration. The section illustrates the breadth and depth of bio-inspired aerodynamics, showcasing examples where biomimicry has been successfully applied, such as wing design inspired by birds' feathers or surface textures derived from shark skin.

Additionally, challenges inherent in translating biological principles into engineering solutions are discussed. The complexities of scaling, material limitations, and adaptability to different operating conditions pose formidable obstacles. Yet, researchers persevere, driven by the potential benefits of improved efficiency, reduced fuel consumption, and minimized environmental impact. The methodologies section concludes by emphasizing the need for a holistic and collaborative approach, bringing together experts from biology, engineering, and materials science to unlock the full potential of bio-inspired aerodynamic design.

This introduction sets the stage for the expected contributions and implications of bio-inspired aerodynamics. As researchers delve into the complexities of biomimicry, they anticipate not only enhanced aerodynamic performance but also the development of innovative design principles that may transcend traditional engineering constraints. The integration of bio-inspired surfaces into vehicles has the potential to reshape industries, offering a pathway to sustainable and energy-efficient transportation. This section also underscores the broader societal and environmental impact of bio-inspired aerodynamics. The reduction of drag and improvement in efficiency could translate into decreased fuel consumption and emissions, aligning with global efforts to combat climate change. As industries increasingly recognize the urgency of sustainable practices, the bio-inspired design of aerodynamic surfaces emerges as a beacon of innovation.

2. Methodology

The compatibility of a suitable model that can be utilized and copied is one of the challenges that arises when attempting to integrate biomimicry with the aerodynamics of a vehicle. Quite frequently, the process of lowering the amount of aerodynamic and hydrodynamic drag entails lowering the amount of frontal area that the flow is confronted with. As shown in a

ISSN: 2278-4632
Vol-10 Issue-11 No.03 November 2020

presentation by Choi [5], this is something that is often seen in fish. Fish have a tendency to be long and skinny, which helps to lessen the amount of pressure drag they experience. Additionally, they feature distinctive skin surfaces that lessen the friction that is connected with the skin. Such geometries, on the other hand, are not very useful for emulating in the field of vehicle aerodynamics." As a matter of fact, this does not apply to all species. The body geometries of many species of fish belonging to the family Ostraciidae are, in point of fact, rather distinctive. This family of fish, the Ostraciidae, has a number of species that are not suitable for use as models since they have been optimized for purposes other than hydrodynamic drag. A good illustration of this is the Horn-Nosed boxfish, which Randall [6] managed to catch. It is not desirable in terms of vehicle design to have an additional "horn" like front, despite the fact that it is a member of the same family. The yellow boxfish, on the other hand, has a very straightforward box geometry that does not include any other geometric elements, which is a desirable characteristic for vehicle imitation. Therefore, a yellow boxfish form has been chosen for the purpose of analyzing its aerodynamic behavior, particularly its drag, via the use of computational fluid dynamics (CFD) modeling as well as experimental research conducted in a wind tunnel.

In order to simulate a wide variety of forms, including road vehicles, contemporary CFD modeling approaches, in conjunction with the growing capabilities of computational computing, are becoming an increasingly practical device. In addition to this, it provides an alternate instrument to the expensive wind tunnel testing. Nevertheless, the data from the wind tunnel are still necessary in order to corroborate the conclusions of the CFD modeling. RMIT's Industrial Wind Tunnel was used for the purpose of conducting the experimental investigation. It has a rectangular test section that is 6 square meters in size, with dimensions of 3 meters in width, 2 meters in height, and 9 meters in length. Approximately 145 kilometers per hour is the greatest wind speed that may be expected in the test portion. The article by Alam et al. [7] has further information on the tunnel. It was planned and made to be a physical replica of a simplified boxfish. Using Styrofoam, the model was constructed. To hold the model while concurrently measuring all three forces (drag, side, and lift/down forces) and three moments (yaw, roll, and pitch), a device was designed that was equipped with a six-component force sensor. This sensor was manufactured by JR3 Inc. in the United States. Wind speeds ranging from 20 to 100 kilometers per hour were used to measure the aerodynamic drag forces, with each wind speed incrementing by 10 kilometers per hour. In order to calculate the drag coefficient (CD), the drag forces were transformed into a non-dimensional parameter. To determine the aerodynamic drag coefficient (CD) and the Reynolds number (Re), the following formulas are used: In this particular piece of writing, neither the lift nor the side forces, nor their respective coefficients, were calculated or provided. Only data pertaining to drag is shown here. In order to represent the airflow that was around the sculpture, the CFX (version 14.5) was used. Through the use of CATIA, a CAD model was generated. The flow surrounding the CAD model was modeled using two different turbulence schemes, namely the normal k-Ʀ scheme and the k-İ method. The procedure of mimicry was used in order to successfully complete the preparation of the

ISSN: 2278-4632
Vol-10 Issue-11 No.03 November 2020

simplified boxfish model for computed fluid dynamics modeling. In order to provide a baseline for the simplified model, a particular yellow boxfish was used, as can be seen in Figure 1(a). In order to simplify the process, the boxfish model was idealized by starting with the actual yellow boxfish and then adding idealization to it. This was done in order to successfully develop the model. When looking at the front and back of the model, which are the areas where the mouth and tail of the fish are placed, the idealization of the model was most obvious. These were perfected and integrated into the main body, which was copied with as much precision as was feasible. Because of the process of converting files, great attention was paid to designing a computational fluid dynamics (CFD) model that was as similar to a computer-aided design (CAD) model as feasible. This was accomplished by selecting the appropriate conversion parameters. Following the incorporation of the model into the idealized wind tunnel test section in the CFD domain, the environment of the wind tunnel was modeled by including the stationary simplified boxfish model

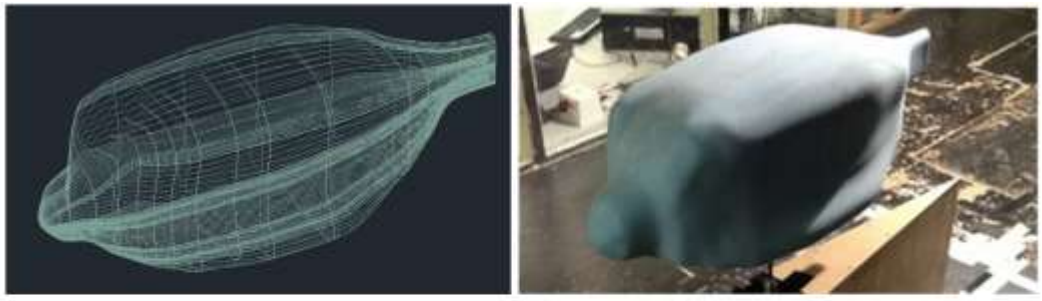

Fig. 1. (a) computational model; (b) wind tunnel model.

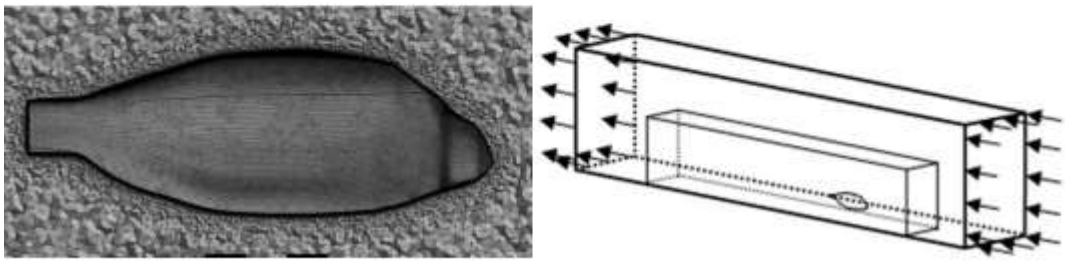

Fig. 2. (a) generated mesh for boxfish model; (b) schematic setup of half model tests.

Due to symmetry, the wind tunnel environment was cut in half for the purpose of conducting the Reynolds number sensitivity tests, as shown in Figure 1. This enabled for much shorter simulation durations to be accomplished, as well as the possibility of additional local mesh refinement in close vicinity to the simpler boxfish model. In addition, the experiments were repeated using the geometry of a full-scale wind tunnel for the sake of comparison. Figure 1(b) shows the model of the wind tunnel as well as the setup for it. The approach of all computational work makes use of a hybrid mesh that is comprised of unstructured triangular and tetrahedral mesh, and it is used over the whole of the wind tunnel environment. For the purpose of more accurately predicting flow separation and flow phenomena in close vicinity to the boxfish model,

ISSN: 2278-4632
Vol-10 Issue-11 No.03 November 2020

an extra layer with a finer surface mesh has been added to the part of the boxfish model that is located on the surface. In addition, a box of influence is included into the environment of the wind tunnel. This is done in order to efficiently distribute finer mesh to the area where flow phenomena need to be examined with more precision. The meshing configuration for the Reynolds number sensitivity tests can be shown in Figure 2. When it comes to the yaw test, a similar method is used. Due to the fact that the box of influence has a far higher concentration of mesh, any extra flow assessment and simulation time in areas that are further away from the sides of the boxfish model is significantly reduced.

Different meshing approaches were developed for both the inflation layer and the box of influence in order to fulfill all of the requirements of both turbulence models. In the case of k-æ, the mesh was reduced in order to minimize the mesh size increase as much as possible. This was done because the first layer height needed to be relatively small in order to achieve the desired y+ for the turbulence model. This table provides a summary of the parameters that were used for both the turbulence models and the related meshes, and the configuration. In order to satisfy all requirements of both turbulence models, different meshing approaches were made for both the inflation layer and box of influence, in the case of k-Ȧ, the mesh was reduced in order to minimize the mesh size increase as much as possible, due to the small first layer height required to achieve the desired y+ for the turbulence model. The settings used for both turbulence models and respective meshes are summarized in Table 1, and the setup in Fig. 2(b).

3. Results

The drag coefficient convergence characteristics of the simplified boxfish model for the conventional k-ð turbulence model are shown in illustration 3(a). All of the experiments were carried out at inflow velocities ranging from 20 to 100 kilometers per hour, which corresponds to the Reynolds number, as visually shown in Figure 3. A clear convergence was detected when the mesh was refined to 8 million elements, as shown in Figure 3(a). It was essential to achieve this convergence in order to raise the confidence that one would acquire a valid result based on the turbulence model that was chosen. It was essential to accomplish this convergence to the maximum possible computational mesh number, which was around 9 million elements of unstructured mesh. This was in addition to meeting the y+ criteria for the turbulence model that was used throughout the process. In Figure 3(b), the variance between the mentioned stable scenario (50 layers) and the non-stable case (30 layers) is shown. Additionally, k-ð and the data from the wind tunnel that is presently accessible are also displayed. It was observed that the two turbulence models had varied degrees of variation in their predictions, as shown in Figure 3(b). Although it was discovered that k-ð underpredicted CD at lower Re numbers, k-¸ overpredicted CD at lower Re numbers. However, there are some uncertainties about the accuracy of the wind tunnel that was employed for lower Re values. In the majority of instances, the k-æ model predicted the outcomes somewhat more accurately than the k-ð model. However, because of its lengthy calculation time, it was less efficient when comparing the accuracy and simulation time of the two turbulence models that were used. In addition, it was discovered that the data from the

ISSN: 2278-4632
Vol-10 Issue-11 No.03 November 2020

wind tunnel more closely matched the less stable k-æ scenario. This case had not completely converged to the 10-5 residual objective, and during this time, the CD had also been somewhat more unstable. It is possible that the greater drag readings for the majority of Re number situations may be explained by the high chance of discrepancies in wind tunnel environments as well as faults or restrictions in the equipment.

In addition to the numerical data, the findings of the post-analysis were investigated further in order to investigate the flow characteristics around the simplified model. Figures 4 and 5 illustrate the flow characteristics that are located all over the model. Both of the primary approaches that the simplified boxfish model uses to obtain reduced drag characteristics are seen in Figure 4. In the front view, there is a transition of the inflow into four major parts; the distinctive form enables a transition into the rear view with very little flow separation, which is mostly evident at the idealized mouth region, which was also discovered to be a zone of improvement that may lead to decreased carbon dioxide levels. There are three vortices formed on each side, which are typically undesirable but are shape specific. The back view reveals that these vortices are produced. From the perspective of the rear view, the primary decrease in drag is accomplished by the diffusion process from all sides. This process effectively contributes to the pressure recovery of the flow and reduces the coefficient of displacement. A representation of the flow characteristics of the airflow around the simplified model may be seen in Figure 5(a). The flow is made possible by the acute rear diffusion angle.

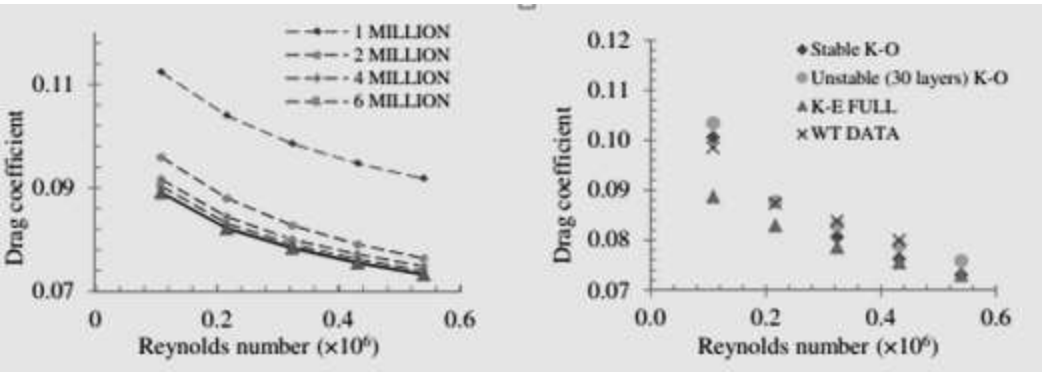

Fig. 3. (a) drag coefficient convergence characteristics; (b) drag coefficient variation with Reynolds number.

The features of the flow of air around the simpler model are shown in Figure 3(a). The flow separation is unavoidable, even when the Re number is 0.1 × 106, because of the extreme rear diffusion angle. Figure 3(b) illustrates the static pressure characteristics at a Re number of 0.1 × 106, which is comparable to the characteristics shown in Figure 5(a). During the process of pressure recovery, there is a diffusion zone situated at the back of the simplified model. It is possible to see that there are regions of relatively high pressure that are positioned close to the idealized region.

ISSN: 2278-4632
Vol-10 Issue-11 No.03 November 2020

4. Conclusion

An investigation into the drag characteristics of a simplified boxfish model was carried out, and the results revealed that a geometry that is comparable to that of a boxfish had highly favorable drag characteristics for a bluff geometry; this was discovered. Combined with the data that is currently available from wind tunnels and mesh convergence studies, computational fluid dynamics (CFD) has made it possible to investigate the flow characteristics of the simplified model. Together with these studies, confidence in the CFD results has been established. Despite the fact that there is a slight variation between the two standards, k-, and k-İ, an overall agreement has been achieved at higher Reynolds numbers. At Reynolds values that were corresponding to an inflow velocity of 100 kilometers per hour, the simplified model had a drag coefficient that was beneficial, measuring 0.073. It was discovered that the boxfish shape was particularly effective in reducing the amount of flow disturbance that occurred through the material that was being studied.

5. References

[1] S. Peter, J.H.K.S. Fiske, Lean, Light and Quiet: Advances in Automotive Energy Efficiency through Biomimetic Design. SAE International, SAE Technical Paper. (2008-21-0028).

[2] M.P. Zari, Biomimetic approaches to architectural design for increased sustainability, School of architecture, Victoria University, NZ, 2007.

[3] European Automobile Industry Report2009/2010. ACEA: www.acea.be [accessed on 10 December 2011].

[4] W.H. Hucho, Aerodynamics of Road Vehicles, 4th ed., SAE International, USA, 1998.

[5] H. H. Choi, H. Park, W. Sagong, Biomimetic flow control based on morphological features of living creatures, Physics of Fluids, 24 (2012) 121302.

[6] J.E. Randal, Ostracion rhinorhynchos, Fishbase.org, [accessed on 10 December 2011]

[7] F. Alam, G. Zimmer, S. Watkins, Mean and time-varying flow measurements on the surface of a family of idealized road vehicles, Experimental Thermal and Fluid Sciences. 27 (2003) 639-654.